

PDZ domain of neuronal nitric oxide synthase recognizes novel C-terminal peptide sequences

Nicole L. Stricker¹, Karen S. Christopherson³, Byungdoo A. Yi³, Peter J. Schatz⁴, Ronald W. Raab⁴, Glenn Dawes⁴, Douglas E. Bassett, Jr.², David S. Bredt³, and Min Li^{1*}

¹Departments of Physiology and Neuroscience, ²Department of Molecular Biology and Genetics, Johns Hopkins University School of Medicine, Baltimore, MD 21205.

³Department of Physiology and Program in Biomedical Sciences, University of California, San Francisco, CA 94143. ⁴Department of Molecular Biology, Affymax Research Institute, Palo Alto, CA 94304. *Corresponding author: (e-mail: min_li@mail.bs.jhu.edu).

Received 2 December 1996; accepted 27 January 1997

PDZ domains are multifunctional protein-interaction motifs that often bind to the C-terminus of protein targets. Nitric oxide (NO), an endogenous signaling molecule, plays critical roles in nervous, immune, and cardiovascular function. Although there are numerous physiological functions for neuron-derived NO, produced primarily by the neuronal NO synthase (nNOS), excess nNOS activity mediates brain injury in cerebral ischemia and in animal models of Parkinson's disease. Subcellular localization of nNOS activity must therefore be tightly regulated. To determine ligands for the PDZ domain of nNOS, we screened 13 billion distinct peptides and found that the nNOS-PDZ domain binds tightly to peptides ending Asp-X-Val. This differs from the only known (Thr/Ser)-X-Val consensus that interacts with PDZ domains from PSD-95. Preference for Asp at the -2 peptide position is mediated by Tyr-77 of nNOS. A Y₇₇D₇₈ to H₇₇E₇₈ substitution changes the binding specificity from Asp-X-Val to Thr-X-Val. Guided by the Asp-X-Val consensus, candidate nNOS interacting proteins have been identified including glutamate and melatonin receptors. Our results demonstrate that PDZ domains have distinct peptide binding specificity.

Keywords: neurotoxicity, NO, PDZ, peptide display

Modular PDZ domains, which have also been called GLGF repeats and disks-large homology repeats (DHRs), consist of about 80 amino acids. These domains were first identified as repeated sequences in the neuron-specific postsynaptic density protein (PSD-95/SAP-90), the *Drosophila* septate junction protein disks-large (dlg), and the epithelial tight-junction protein zona occludens-1^{1,2}. PDZ domains are found in structural proteins of the cytoskeleton and in a heterogeneous family of enzymes that associate with the cytoskeleton, suggesting a role in protein-protein interactions³. Supporting this notion, the three PDZ domains within PSD-95 were first shown to bind the carboxy-terminal Ser/Thr-X-Val motif found in certain N-methyl-D-aspartate (NMDA)-type glutamate receptors and in Shaker-type potassium channel subunits^{4,5}. Clustering and localizing channels at synaptic sites is one function of the concatenated domains⁶.

The crystal structures of the third PDZ domains of PSD-95 and dlg have been determined^{7,8}. The PDZ structures show a carboxylate binding loop containing the signature GLGF sequence, which interacts with the C-terminal carboxylate group of the peptide ligand. The peptide ligand forms main chain interactions with backbone amide groups in a conserved α helix and β strand of the PDZ domain. A critical sequence-specific interaction has been noted between the threonine at the -2 position of the bound peptide and a histidine residue in the PDZ domain⁷. This histidine is conserved in all PDZ repeats of dlg, PSD-95, and related proteins. However, it is not conserved in other PDZ domains³, suggesting distinct peptide-binding specificities.

PDZ domains mediate specific protein-protein interactions. Thus, understanding the biological function of PDZ-containing proteins will necessitate determining the physiological ligand(s)

for orphan PDZ domains. The interaction between the PDZ domain and peptide ligands can be regulated by differential affinity⁹ and by protein phosphorylation¹⁰. These mechanisms, however, are not adequate to explain the diversity of PDZ-target protein interactions in both excitable and nonexcitable tissues.

Nitric oxide (NO), an endogenous signaling molecule, plays critical roles in nervous, immune, and cardiovascular function¹¹⁻¹³. Although there are a variety of functions for neuron-derived NO, which is produced primarily by the neuronal NO synthase (nNOS), excess nNOS activity mediates brain injury in cerebral ischemia and in animal models of Parkinson's disease¹⁴⁻¹⁶. nNOS activity must therefore be tightly regulated. Indeed, a protein inhibitor of nNOS has recently been described¹⁷. A more complex level of regulation is reflected by molecular targeting of nNOS to specific intracellular membrane domains¹⁸. This subcellular localization is mediated by the N-terminus of nNOS, which contains a PDZ domain¹⁹. This N-terminal domain of nNOS interacts with the PDZ domain of α 1-syntrophin and the second PDZ domains of PSD-95 and PSD-93. These interactions target nNOS to synaptic sites in skeletal muscle and brain²⁰. The structural details of these PDZ-PDZ interactions are not yet known.

Several lines of evidence suggest that additional binding partners for the PDZ domain of nNOS may also exist. Not all membrane-associated nNOS in brain is bound to PSD-95 and related proteins²¹. In certain muscle diseases, nNOS does not interact properly with α 1-syntrophin at the skeletal muscle sarcolemma²². We therefore sought to determine whether specific carboxylate-peptides might associate with the PDZ domain of nNOS. Identification of such peptides would facilitate the structure and function study of PDZ domains. Also, the in vitro identified peptide

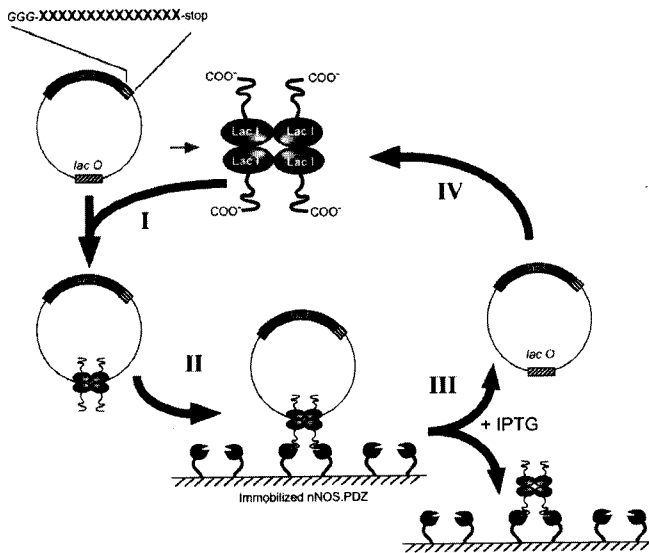


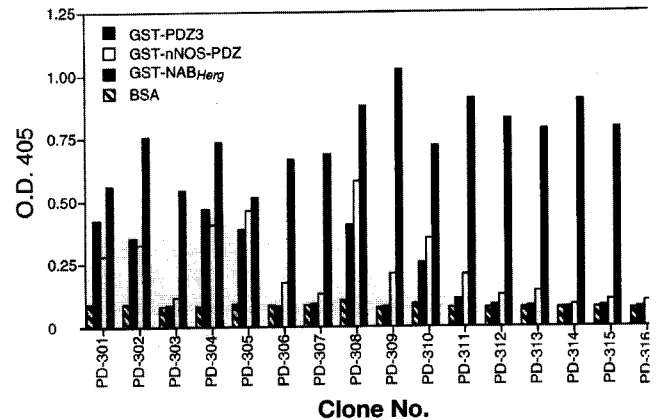
Figure 1. Affinity selection from a C-terminal peptide library. (I) A pool of oligonucleotides encoding 15 random amino acids (X_{15}) was cloned in frame C-terminal to *lac I*. Protein expression from each plasmid of the library yields a Lac I fusion with a distinct peptide sequence. The recombinant Lac I binds the *lac O* sites present on the same plasmid yielding Lac I-plasmid complexes that are purified from the *E. coli*. (II) Affinity panning selects peptides that interact with target receptor (i.e., PDZ domain of nNOS.) (III) The bound plasmid DNA can be specifically recovered by addition of isopropyl β -D-thiogalacto-pyranoside (IPTG). (IV) The recovered plasmids are retransformed, amplified, and used for subsequent rounds of panning.

sequences may help identify additional nNOS interacting proteins.

In vitro determination of ligands for peptide-binding domains, such as SH3 and SH2 motifs, has been achieved using two types of random peptide libraries²³⁻²⁵. One strategy utilizes the filamentous phage coat protein to display random N-terminal peptides. By repeated rounds of affinity panning and amplification, individual interacting peptides can be identified by sequencing the corresponding coding region of phage DNA²³. A second approach uses soluble random peptides that are chemically synthesized. By affinity purification of a mixture of bound peptides and subsequent peptide sequencing, a population-based consensus can be deduced²⁴. Because the phage display system only accommodates N-terminal peptides, it can not be used to select C-terminal peptides for the PDZ domain. Although chemical peptide libraries are applicable, the approach has difficulties in accommodating cysteine and tryptophan and does not provide individual ligand sequences. As a result, analyses of chemical libraries cannot resolve compensatory effects potentially present in peptides of low abundance and may miss high-affinity sequences containing tryptophan and cysteine. Thus, it would be desirable to use a genetic strategy to screen a large pool of C-terminal peptides containing all 20 amino acids to identify individual PDZ binding peptides.

We have taken advantage of a C-terminal peptide display strategy²⁶ and screened 13 billion distinct C-terminal peptides to select sequences specific to the PDZ domain of nNOS. Ninety-six sequences have been identified, including individual peptides that bind tightly to the PDZ domain of nNOS. These peptides have a C-terminal consensus sequence of D-X-V-(COOH) and do not bind to the PDZ3 domain present in PSD-95. We suggest that Y_{77} of nNOS determines binding to D at the -2 position of the peptide, and by mutating $Y_{77}D_{78}$ to $H_{77}E_{78}$, we change the specificity of nNOS PDZ from D-X-V to T-X-V. We also find that the nNOS PDZ domain has unique structural features making the functional

A



B

Clone No.	Sequence
Library	GGGXXXXXXXXXXXXXXXXX*
PD-303	GGGRSLIGAVEKRQETSV*
PD-307	GGQETLRLRLSVGPETSV*
PD-312	GGHRRSARYLEESV*
PD-314	GGGREASNKVRRLRKESTV*
PD-315	GGGGPESLLWKVRRRETSL*

Figure 2. Affinity selection of peptides interacting with PDZ3 of PSD-95. (A) Identification of PDZ3 interacting clones by ELISA. Crude bacterial lysates from individual clones (horizontal axis) selected through four rounds of panning were prepared. Association of Lac I-peptide fusion with GST-PDZ3 was determined by ELISA. Dashed bars indicate wells coated with BSA only; gray bars: GST-NAB_{HERG} + BSA; white bars: GST-nNOS-PDZ + BSA; black bars: GST-PDZ3 + BSA. GST-NAB_{HERG} is a fusion protein containing amino acids 1 to 135 from *HERG* potassium channel, which has no homology with PDZ domain³⁶. All ELISA experiments were repeated at least once with similar results. (B) Alignment of deduced amino acid sequences of PDZ3-specific clones. PDZ3-specific clones were chosen and sequenced. Single letter code for 20 amino acids are used. Italic letters indicate amino acids present at the end of the linker, which separates Lac I from the fused peptide. Asterisk, *, indicates stop codon. Some peptides were truncated as the peptide library was constructed using NNK scheme, in which stop codon occurs at frequency of 1/32.

domain larger than that predicted by sequence alignments. Using the consensus binding sequence, we have electronically identified candidate nNOS-interacting proteins.

Results

Construction of a random C-terminal peptide library. Peptide binding and x-ray crystallographic studies of PSD-95 indicate that specificity of the peptide-PDZ interaction is primarily determined by the final four residues of the peptide ligand^{4,5,7,9,27}. To determine optimal peptide binding ligands for other PDZ domains, we constructed a fusion protein library that contains 15 randomized residues at the C-terminus. In this library, a degenerate oligonucleotide encoding the random peptides is fused to the end of the *Escherichia coli lac* repressor²⁶. Following expression, the Lac repressor protein binds to the *lac* operator sequence on the same plasmid linking each randomized 15-mer peptide to the plasmid encoding that peptide (Fig. 1). This linkage allows repeated rounds of selection for specific peptide ligands in the population by affinity purification of peptide-repressor-plasmid complexes.

In vitro selection of optimal binding peptides for PDZ

domains. We first screened a random 15-mer peptide library using the third PDZ (PDZ3) domain of PSD-95. In PSD-95, PDZ1 and PDZ2 domains interact with the C-terminal four amino acids found in Shaker potassium channels and NMDA receptor subunits^{4,5}, which have a shared consensus of E-(T/S)-X-V-COOH. PDZ3 binds to an identical sequence⁷. A PDZ3 fusion protein was constructed by linking amino acids 302 to 402 of PSD-95 to the C-terminus of glutathione S-transferase (GST). The purified protein was incubated with a 15-mer *lac I* library with a complexity of 1.3×10^{10} . After 4 rounds of panning selection, a 1,700-fold enrichment of interacting peptides was achieved. Since GST fusion protein of PDZ3 was used in panning and bovine serum albumin (BSA) was used for blocking nonspecific binding, the selected peptide may interact with the GST portion, the PDZ3 domain, or BSA. In order to identify peptides that are specific for the PDZ3 domain, individual clones were randomly selected and subjected to ELISA analysis using either the GST-PDZ3 fusion or GST-NAB_{HERG}, an unrelated GST fusion protein (Fig. 2A). The enriched clones were divided into two classes. One class, including PD-301, PD-302, and PD-304, interacted with both GST-NAB_{HERG} control and GST-PDZ3

fusion, suggesting that the corresponding peptides interact with GST. The other class of clones, including PD-312, PD-314, and PD-315, bound selectively to GST-PDZ3. Affinity of interaction (EC₅₀) was 2 to 100 nM as determined by quantitative ELISA.

To determine the binding specificity, purified recombinant PDZ fusion protein of nNOS (amino acids 1 to 150)²⁸ was tested for peptide binding. Under the same conditions, the PDZ3-positive clones failed to interact with the PDZ domain of nNOS (Fig. 2A). Plasmids encoding PDZ3-specific clones were sequenced. Most of the interacting peptides closely resemble the peptide sequence at the C-terminus of Shaker-like potassium channels and NMDA receptor subunits, with a consensus of E-(T/S)-X-V-COOH (Fig. 2B).

Identification of novel peptides interacting with PDZ domain of nNOS. To determine optimal peptide ligands for the nNOS PDZ domain, a recombinant GST fusion protein corresponding to the coding sequence of amino acids 1 to 150 of nNOS (nNOS-PDZ) was used for peptide selection. After four rounds of panning, a 2,300-fold enrichment was achieved. Individual GST-nNOS-PDZ specific clones were identified by ELISA. Ninety-six out of 150

Table 1. Sequence alignment of nNOS binding peptides (NBP).

Clone no.	Sequence	Clone no.	Sequence
NBP-4	GGGGTPQKAVHRDWGVSV*	NBP-74	GGGDRGWAVGWGLRGVFPV*
NBP-5GGGIRAGGDPV*	NBP-76GGGGPARYGDSV*
NBP-7GGGDPV*	NBP-77GGGDLV*
NBP-8GGGDARTKIWNRAADLI*	NBP-78	GGGFSSSLVLGAGDLGVAP*
NBP-9	GGGAQGRWPQFCVYPDAV*	NBP-79	.GGGMQWVAQRDLAAGDCV*
NBP-10GGGVHVFSDSV*	NBP-81	GGGKDGGRQGANFFGDAV*
NBP-11GGGVLGDLV*	NBP-82GGGTWGRAV*
NBP-12	GGGAMEVTTLSHQPGDPV*	NBP-83	GGGLKSTGSEVNSLGDVIV*
NBP-14GGGDAI*	NBP-84	GGGSEATAVWTSKWSDLV*
NBP-15	GGGWAGYGRGMVAVSGDMV*	NBP-85	GGGPVSSVRYSGVAGDQV*
NBP-17	GGGFPFFMGTMGEGYGIQV*	NBP-86GGGLWSDAV*
NBP-18	GGGLGKDYPSAPDNGDLV*	NBP-87	GGGRVTGRSSYLGMGDIV*
NBP-24	GGGIYGMRIQTGLVDVL*	NBP-88GGGDMV*
NBP-27	GGGAGQDKAQAGQHWGDLV*	NBP-89	GGGKFSVRHTLVSAGDPV*
NBP-28GGGGVDWV*	NBP-91	GGGARGQLPATRCKAFLC*
NBP-32GGGDAV*	NBP-92GGGYEEGVAV*
NBP-33GGGRWDWV*	NBP-93GGGDRV*
NBP-34	GGGKGHIAITSDGVGDLL*	NBP-94GGGDLV*
NBP-35	GGGNYDRVGLLRGPVDFL*	NBP-95	GGGVRGALTRGMTPGDPV*
NBP-36	GGGKRPDGVLFQRPGDLV*	NBP-96GGGDLV*
NBP-37GGGDAV*	NBP-102	...GGGVAVGVKYGDLV*
NBP-41GGGDPV*	NBP-103GGGDLV*
NBP-42GGGDAV*	NBP-107GGGDLV*
NBP-44	GGGGLARLNLSSYYGDAV*	NBP-108GGGKMRVGVDAV*
NBP-45GGGVDWV*	NBP-111GGGDPV*
NBP-47	GGGRVIGSPNPSRSADIV*	NBP-112GGGRDSERLMGIPIV*
NBP-48GGGDWV*	NBP-113GGGDQV*
NBP-49	GGGSFMNBPVAGTAGDSV*	NBP-114GGGRWSEGDGV*
NBP-52GGGSRGDMV*	NBP-117	GGGLGRGSRVPRRRPDIIV*
NBP-53GGGDWV*	NBP-118GGGDVIV*
NBP-54	GGGDGMLLRPQLRWIFC*	NBP-119	GGGIKRLDIYMRNIGDLV*
NBP-55	.GGGKRDETFGNMWNNAV*	NBP-122GGGSATAWNGDFV*
NBP-56GGGWQGDPV*	NBP-123	.GGGLDRLRNRVHGDVAV*
NBP-57GGGGALGDPV*	NBP-124	GGGREVSVCHRPDAGDAV*
NBP-59GGGDPV*	NBP-125	GGGSRVPRNTSIFWGNVAV*
NBP-60GGGDLV*	NBP-126	GGGDCGNVTHAILWGDVAV*
NBP-61GGGESGSGVRTWGVFPV*	NBP-128	GGGKALGAIYVMGGVDVAV*
NBP-62GGGRVQLVRGGVDCV*	NBP-129GGWGSFPV*
NBP-64GGGDAV*	NBP-131	GGGKGSPSLVGPVWADAV*
NBP-65	.GGGWRVVKVSMRWPDPV*	NBP-133	GGGILNVPVPRNLSEGDVIV*
NBP-66GGGDLV*	NBP-136GGGDQV*
NBP-67GGGSKSCGRVILGDIV*	NBP-137	GGGGERLNRSATAGADLV*
NBP-68GGGVDWV*	NBP-138GGGEGRRNPDIIV*
NBP-69	GGGIIQGQARGTRWEMV*	NBP-140	GGGNQRYVNVNPFIFWQQSV*
NBP-70GGGDAV*	NBP-142GGGDSINLSWFPVAV*
NBP-71	GGGGGWPELNPNLGLVPI*	NBP-143	GGGCMLQVRHIYGPCDAV*
NBP-72	GGGRCMLNLVTRWADTV*	NBP-161GGGVIGKSCYGDVAV*
NBP-73	GGGGMGQTLLEELTTGDWV*	NBP-226GGCAVSPDFGDVAV*

Sequence alignment of 96 independent NBPs. The deduced amino acid sequences of 96 independent clones were obtained and aligned according to the first stop codon (*). The italic Gs are part of the linker region. The library template is GGG-XXXXXXXXXXXXXXXXXX*.

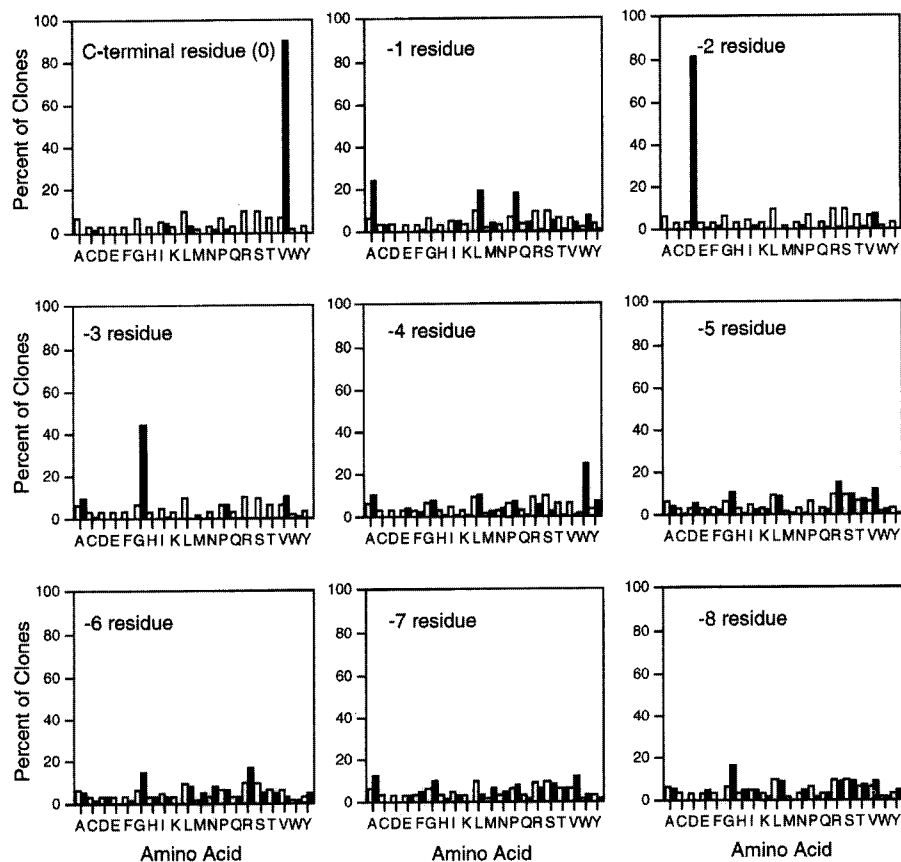


Figure 3. Determination of a consensus nNOS binding peptide (NBP). Normalized amino acid abundance of the final nine residues from the population of 96 independent nNOS binding peptides (black bars) is compared with codon frequency in the original library (white bars). Residues in the library linker region were not included.

clones specifically interacted with nNOS-PDZ but not with the control GST fusion protein. Binding affinity of these peptides to immobilized nNOS-PDZ (EC_{50}) was 8 to 100 nM. Plasmids from these nNOS-specific clones were sequenced. The deduced amino acid sequences of 96 independent clones were aligned via their C-termini (Table 1).

An analysis of amino acid abundance at each position indicates that valine again is strongly preferred (89%) at the 0 position (Fig. 3). At the -1 position, there is no obvious preference. Fifteen of the 20 amino acids were found; amino acids D, E, H, K, and N were not present. In contrast to the PDZ3 consensus, aspartate at the -2 position was present in 81% of all nNOS-PDZ binding peptides. At the -3 position, glycine is significantly preferred. Considering that glycine was used as a part of the linker that separates Lac I from the random peptide (Fig. 1), we appropriately corrected this bias. The corrected glycine abundance is 47% at the -3 position. From position -4 to position -8, no obvious amino acid preference was observed (Fig. 3). Based on the amino acid abundance at each position, the optimal sequence for an nNOS binding peptide (NBP) is D-X-V-COOH.

Specificity of NBP binding to nNOS-PDZ. Our *in vitro* peptide selection suggests that PDZ3 of PSD-95 and the nNOS-PDZ, despite a shared preference for valine at the 0 position, have distinct binding specificity. To directly test this, we performed ELISA and found that 36 randomly chosen NBPs failed to bind to PDZ3 of PSD-95 (Fig. 4A). The higher affinity sequences of NBPs were selected using putative monovalent maltose binding protein fusion²⁹. For example, mNBP161 has an EC_{50} of 8 nM (Fig. 4B). Based on the peptide-PDZ3 crystal structure⁷, the side-chain of His₃₇₂ of PSD-95 forms a critical sequence-specific hydrogen bond with the T at the -2 position of the bound peptide. Interestingly, the amino acid at the corresponding position of nNOS-PDZ is Y₇₇,

consistent with the idea that substitution of H to Y at this position converts the -2 position peptide preference from T to D. Amino acid sequence comparison of a number of PDZ domains present in Genbank shows that the residue after the H or Y is also conserved (nNOS is Y-D, PDZ3 is H-E). To determine whether the Y₇₇ of nNOS is critical, we mutated Y₇₇D₇₈ to H₇₇E₇₈. This mutant, nNOS-PDZ_{H77E}, lost its ability to bind D-X-V peptides and gained the ability to bind T-X-V peptides (Fig. 4C).

To evaluate the specificity of the NBP-nNOS interactions, we mutated the D at the -2 position of the NBP-123 (LDRLRN-RVHGDAV-COOH, EC_{50} = 40 nM) peptide to A, L, Q, R, S, T, and V. Peptides with these amino acid substitutions failed to interact with nNOS-PDZ (Fig. 4D). To test whether NBPs bind to native nNOS protein, we generated an affinity column linking NBP-123 to an agarose matrix. We found that nNOS protein in crude rat brain homogenates adhered to the NBP-123 matrix. In contrast, nNOS did not bind to an analogous column in which the -2 D residue of NBP-123 was mutated to T (Fig. 4E).

The nNOS-PDZ domain has unique structural features. Previous studies have shown that the N-terminal domain of nNOS (amino acids 1 to 150) binds to the PDZ domain of α 1-syntrophin and to the second PDZ domains of PSD-95 and PSD-93 (ref. 20). Although amino acids 16 to 100 of nNOS define the consensus PDZ domain, binding studies have shown that fusions containing amino acids 1 to 100 of nNOS do not bind to the PDZ domain of either α 1-syntrophin or PSD-93 (ref. 20). To determine whether the peptide binding property of the nNOS-PDZ is confined to the typical consensus, we tested whether any of five randomly selected NBPs interact with a fusion protein containing nNOS 1 to 100. All five NBPs bind to nNOS (1 to 150) but not to nNOS (1 to 100) (data not shown).

To determine the minimal functional structure for nNOS-

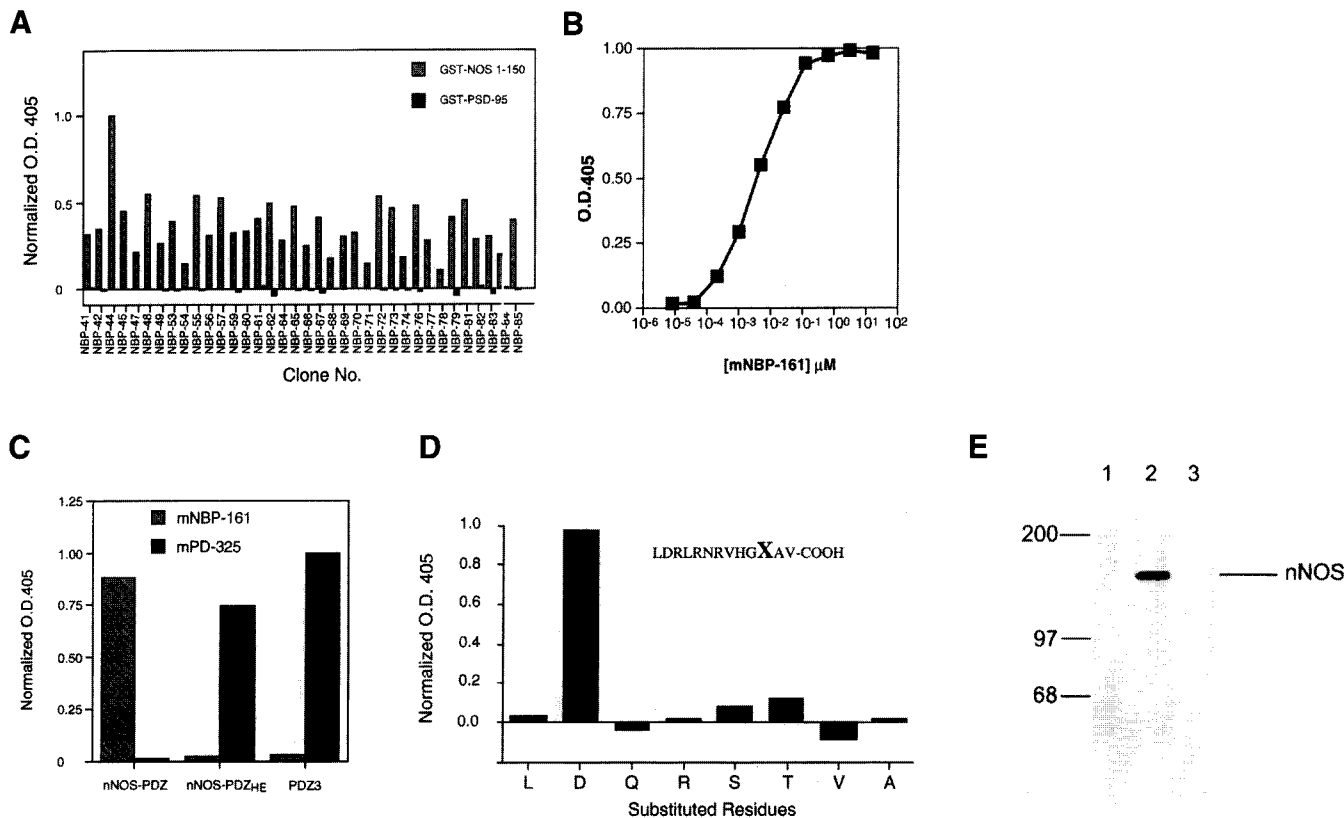


Figure 4. NBPs bind specifically to nNOS PDZ and native nNOS protein from rat brain. (A) ELISA results of 36 randomly chosen NBP clones. Horizontal axis: NBP clone number; vertical axis: ELISA signal normalized against the clone with strongest binding (NBP-44). (B) Dose-response curve of mNBP-161 binding to GST-nNOS-PDZ. The binding was performed using maltose binding protein fusion of NBP-161 (Table 1). The EC₅₀ of mNBP-161 was estimated using the Hill equation. (C) Mutating Y₇₇D₇₈ to H₇₇E₇₈ changes the nNOS PDZ binding specificity from D-X-V to T-X-V. ELISA results of two high-affinity peptides are shown. The maltose binding protein fusions of NBP-161 (or mNBP) for nNOS (EC₅₀ = approximately 8 nM) and PD-325 (or mPD-325) for PDZ3 (EC₅₀ = 2 nM) were expressed in *E. coli*. (D) The aspartate at the -2 position is critical for NBP binding. Single amino acid substitutions at the -2 position were engineered, and the peptides were expressed as maltose binding protein fusions. ELISA results from seven mutants are shown. (E) Solubilized brain extracts were incubated with amylose resin alone (lane 1), amylose resin saturated with a maltose binding protein fusion containing a C-terminal NBP-123 (lane 2) or with the same fusion protein in which the -2 aspartate was changed to threonine (lane 3). The beads were washed and retention of nNOS was detected by Western blot analysis. Molecular weight standards in kDa are marked on the left.

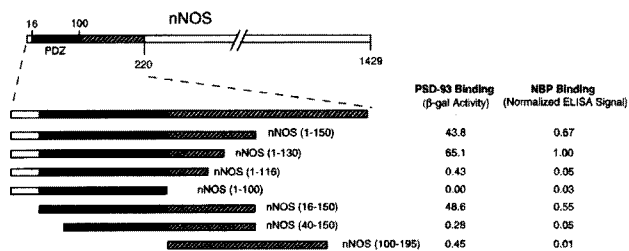


Figure 5. The functional nNOS PDZ has a uniquely large structure. Interaction of nNOS with the PDZ domains of PSD-93 requires amino acids 16 to 130 of nNOS. Top: a schematic diagram of the N-terminus of nNOS showing the location of the PDZ domain. Bottom: association of nNOS fusions with PSD-93 was evaluated by the yeast two-hybrid system and is expressed as β -galactosidase units. Interactions of five different NBPs (#64 to 68) with nNOS fusions were evaluated by ELISA and are expressed as normalized OD₄₀₅.

PDZ to bind NBPs and PSD-93, we generated a panel of six fusion proteins that express various regions of the N-terminus of nNOS (Fig. 5). We first evaluated binding of these constructs to the PDZ repeats in PSD-93 using the yeast two-hybrid analysis. Binding to PSD-93 required amino acids 16 to 130 of nNOS; truncations on either side of this core nNOS-PDZ eliminate the

interaction. Similarly, all NBPs required amino acids 16 to 130 for binding as tested by ELISA (Fig. 5). These studies indicate that the functional nNOS-PDZ requires additional amino acids beyond the conserved consensus and indicate that both peptide-PDZ and PDZ-PDZ interactions of nNOS likely require a similar tertiary structure.

Candidate proteins that interact with nNOS. Identification of the ligand binding consensus of nNOS-PDZ allows a search for potential nNOS interacting proteins present in the protein databases possible. A prerelease version of the XREFPatScan software was used to find the D-X-V pattern at the carboxy-terminus of protein sequences in the nonredundant protein database maintained at the National Center for Biotechnology Information (<http://www.ncbi.nlm.nih.gov>). This sequence pattern scan showed 484 matches in the database (available from our web site: <http://physiology.med.jhu.edu/min/min.html>). Interestingly, this list of potential binding partners includes both glutamate and melatonin receptors, which are known to influence NO signaling^{30,31}.

Discussion

To identify C-terminal peptide ligands for the nNOS PDZ domain, the strong protein-DNA association between the *lac* repressor and the *lac* operator sequence is used to obtain a complex library of expressed peptides each bound to the plasmid that encodes them.

By simply panning for peptide binding and then sequencing the corresponding plasmids, we were able to rapidly determine optimal binding partners for the nNOS-PDZ. Identified peptides bind to nNOS with binding affinities (EC_{50}) in the 8 to 100 nM range, similar to the affinity of the NMDA receptor for PDZ domains of PSD-95 (ref. 9). These peptide sequences are likely to be physiologically relevant because a similar panning procedure yielded the known peptide ligands for PDZ3 of PSD-95.

The consensus peptide binding sequence for the nNOS-PDZ is D-X-V, which contrasts with the E-(T/S)-X-V found for PDZs of PSD-95 (refs. 4, 5, 7, 9, 27). Analysis of the crystal structure of peptide-bound PDZ3 suggests rational explanations for the alternate specificity⁷. Similar preference of the two domains for terminal valine is expected because the critical residues in the carboxylate binding loop of PDZ3, including the GLGF tetrapeptide, are precisely conserved in nNOS-PDZ. While the carboxylate loop of PSD-95 binds most potently to peptides with C-terminal valine, other terminal hydrophobic amino acids are permitted. Such degeneracy was also found in some nNOS binding peptides, e.g., NBP-14 (Table 1). Inwardly rectifying potassium channel subunits of class 2.0 terminate with E-S-X-I, and these channels also bind to PSD-95. In addition, the -2 serine of Kir 2.3 serves as a potent substrate for protein kinase A, and this phosphorylation event regulates binding of the channel to PSD-95 (ref. 10).

Specificity of PDZ3 for T/S at the -2 position of the peptide is mediated by hydrogen bonding of the hydroxyl of the T/S with the N-3 nitrogen of H₃₇₂ of PDZ3 (ref. 7). The corresponding residue in nNOS is Y₇₇. The greater electrophilic character of Y compared with H may explain the preference of the nNOS PDZ for the acidic amino acid D at peptide position -2. Accordingly, mutation of Y₇₇D₇₈ of nNOS to H₇₇E₇₈ changes the binding specificity from DXV to TXV. Interestingly, the Y₇₇ position is not generally conserved in other orphan PDZ domains, and this single residue may allow for much of the diverse peptide ligand specificity at the -2 position.

These studies emphasize that the nNOS PDZ domain has unique structural features. The consensus PDZ domain contains approximately 80 amino acids, and PDZ3 of PSD-95 was functionally active as a 101-amino acid polypeptide⁷. By contrast, a functional nNOS PDZ domain requires an additional 30 amino acids C-terminal to the identified consensus. We wondered whether the smaller nNOS constructs, such as nNOS 1 to 100, were inactive due to a nonspecific problem with polypeptide folding. However, circular dichroism analysis predicted a high degree of secondary structure for nNOS 1 to 100 (data not shown). Therefore, we believe that the functional nNOS PDZ has a structure somewhat larger than that of other PDZ domains. By using our genetic peptide selection strategy, it will now be possible to determine whether other PDZ domains are also larger than the presently identified consensus.

In addition to interacting with peptide ligands, the PDZ domain of nNOS associates with other PDZ domains, including the PDZ domain of α 1-syntrophin and the second PDZ of PSD-95 and PSD-93 (ref. 20). The three-dimensional structure of a PDZ / PDZ heterodimer is not yet available, but our data is consistent with the idea that the PDZ / PDZ binding interface overlaps with the peptide recognition sequences. Thus, deletions of nNOS PDZ that abolish peptide binding also eliminate binding to α 1-syntrophin and PSD-93 (Fig. 5). Crystallography of PDZ3 of dlg showed that the PDZ domain forms a dimer in which the surface of the peptide-binding domain of one PDZ subunit interacts with residues in β -strands from the other subunit⁸. This binding topology of PDZ domains may explain why the SXV peptide of the NMDA receptor 2B potentially blocks nNOS binding to PSD-95 (ref. 20). Proteins containing the DXV nNOS interacting domain may also disrupt interaction of nNOS with PDZ proteins. This may

explain the paradoxical situation that α 1-syntrophin, but not nNOS, is present at the sarcolemma in patients with Becker's muscular dystrophy²². Perhaps, in the myofibers of these patients, the nNOS PDZ is occupied by a protein with a C-terminal D-X-V and is unable to bind to α 1-syntrophin.

A protein database search, with the terminal DXV consensus for nNOS, yielded several attractive binding partner candidates including melatonin receptor 1a (U14108) and an alternatively spliced form of GluR6 (X66117). Though nNOS is best activated by calcium influx through NMDA receptors³⁰, NO signaling can also be regulated by melatonin³¹ and by non-NMDA type glutamate receptors³². Our data suggest that physical association of nNOS with GluR6 and with melatonin receptors may participate in this functional coupling.

Experimental protocol

Fusion protein expression and purification. GST-fusion proteins were expressed in either DH5 α or BL21 bacterial strains. Cultures with an OD₆₀₀ of 0.2 were induced for three hours with isopropyl β -D-thiogalactopyranoside (IPTG). Bacteria were harvested by centrifugation and resuspended in 10 ml of NETN buffer, which contains 20 mM tris(hydroxymethyl)aminomethane (Tris), pH 8.0, 100 mM NaCl, 1 mM ethylenediamine tetraacetic acid (EDTA), 0.5% NP-40, and 2 mM phenylmethylsulfonyl fluoride (PMSF). The bacterial cells were lysed by sonication. Affinity purification using glutathione-sepharose beads was carried out according to protocols provided by the manufacturer (Pharmacia Biotech, Uppsala, Sweden).

Library construction. The random 15-mer library was constructed as described in detail by Schatz et al.²⁹ using an oligonucleotide with a degenerate region of 15 codons in the form of NNK, where N denotes an equimolar mix of all four bases and K denotes a mix of G or T. The library consisted of 1.3×10^{10} independent recombinants. The amplified library was stored at -80°C in HEK buffer containing 35 mM HEPES pH 7.5, 0.1 mM EDTA, and 50 mM KCl.

Construction of maltose binding protein fusions. Nucleotide sequences encoding appropriate peptides were cloned into pELM3²⁹. This allows expression of the corresponding maltose binding protein/peptide fusion. The procedure for expression of maltose binding proteins was identical to that for GST fusions except that the LB medium was supplemented with 2% glucose.

Affinity panning. A 2-ml aliquot of thawed bacterial cells in HEK was added to 6 ml of lysis buffer 25 mM HEPES pH 7.5, 0.07 mM EDTA, 8.3% glycerol, 1.25 mg/ml BSA, 0.83 mM DTT, 0.2 mM PMSF. The bacteria were lysed for 2 to 4 min on ice by the addition of 0.15 ml 10 mg/ml lysozyme (Boehringer Mannheim, Indianapolis, IN), and then 2 ml of 20% lactose and 0.25 ml of 2 M KCl were added. The supernatant was obtained after a 15-min centrifugation at 27,000 \times G. To initiate panning, 12 wells of a 96-well plate were first coated with GST-fusion proteins (10 μ g protein per well) at 4°C for 1 h. The wells were then blocked with 1% BSA in phosphate-saline buffer (PBS) at pH 7.4. After precoating, 250 μ l of the supernatant was added to each of precoated wells. After gentle agitation for 1 h at 4°C, the unbound material was recovered, and the wells were then washed with a series of solutions: five times with HEK buffer supplemented with 0.2 M lactose and 1% BSA, twice with HEK supplemented with 0.2 M lactose, and twice with HEK at 4°C. The bound plasmids were eluted with 35 mM HEPES pH 7.5, 0.1 mM EDTA, 200 mM KCl, 1 mM IPTG for 30 min at room temperature. The eluted DNA was precipitated with isopropanol and amplified by electrotransformation. This pool of bacterial transformants were used in subsequent rounds of panning. The panning procedure was monitored by two parameters: percent recovery and enrichment. Recovery was calculated by dividing the number of plasmids at the beginning of panning (input) by the number of plasmids bound to BSA-coated wells (output). The enrichment at each round of panning was the ratio of recovered plasmids from receptor-coated wells to those recovered from BSA-coated wells.

ELISA. After three to four rounds of affinity panning, individual colonies were randomly selected. Overnight cultures from single colonies were diluted 1:10 in 3 ml of LB ampicillin (100 μ g/ml) and grown 1 h at 37°C. The expression of the LacI-peptide fusions was induced by the addition of arabinose to 0.2% for 3 h. After induction, the cells were pelleted by centrifugation and lysed as described above in 1 ml of lysis buffer plus lysozyme. The clarified lysates were used immediately for ELISA or stored at -70°C. To prepare

ELISA, 96-well plates were first coated with GST-fusion proteins (0.2 µg protein per well) of nNOS or PSD-95 at 4°C for 1 h. The wells were then blocked with 1% BSA in PBS at pH 7.4. After precoating, the wells were washed three times with PBS supplemented with 0.05% Tween-20 (PBT). To initiate the binding, 100 µl of 1:10 diluted lysate was added to each well. After 30 min at 4°C, the plate was washed four times with PBT. The binding of LacI-peptide was detected using rabbit anti-LacI antibody. After four washes with PBT, the plate was developed by adding alkaline phosphatase-conjugated goat anti-rabbit antibody (GIBCO-BRL, Gaithersburg, MD) in PBS/0.1% BSA (100 µl per well for 1 h at 25°C) followed by a 6-min treatment with p-nitrophenyl phosphate (1 mg/ml) in 1 M diethanolamine hydrochloride, pH 9.8/0.24 mM MgCl₂ (200 µl per well). Binding was quantified by monitoring optical density at 405 nm on an E-max plate reader (Molecular Devices, Menlo Park, CA). The negative controls were wells coated with control GST fusion or as otherwise indicated. All experiments were repeated at least once with similar results. ELISAs for maltose binding fusion proteins were performed as described above with a few modifications. 100 microliters of a 1:50 dilution of crude lysate were added to each well. All buffers were the same but were supplemented with 1 mM maltose to minimize oligomerization of maltose binding protein fusions³³. Interaction of maltose binding protein fusion proteins with immobilized GST-fusion proteins was monitored by rabbit anti-maltose binding protein antibody (1:10,000 dilution, New England Biolabs, Beverly, MA).

Peptide-PDZ binding. To determine the affinity of peptide-PDZ interactions, monomeric maltose binding protein fusions of peptides were purified by amylose affinity columns according to a protocol provided by the manufacturer (New England Biolabs). Protein concentration was determined by the Bradford assay (Bio-Rad, Hercules, CA) using BSA as standard. The effective concentration (i.e., EC₅₀) was determined by dose-dependent ELISA tests. GST fusion was bound at 0.05 µg per well. The maltose binding protein fusions were incubated after being serially diluted (1:5) starting at 15 mM. The data were fit with the Hill equation ($O.D._{405} = O.D._{405\text{ Max}} / (1 + \{EC_{50} / [X]\}^n)$). A nonlinear least square algorithm was used.

Yeast two-hybrid analysis. Yeast Y187 cells were cotransformed with expression vectors encoding various Gal4 DNA binding domain-nNOS fusions and the Gal4 activation domain fused to PSD-93 (amino acids 116 to 421). Each transformation mixture was plated on synthetic dextrose plates lacking tryptophan and leucine. Interaction was measured by the liquid culture β-galactosidase assay as described³⁴ (Clontech, Palo Alto, CA). Values are representative of duplicate experiments.

Fusion protein affinity chromatography. Rat whole brain was homogenized in 10 volumes (w/v) tris-HCl buffer pH 7.4 and centrifuged at 32,000 × G for 20 min. Membranes were solubilized for 2 h at 4°C in buffer containing 200 mM NaCl and 1% Triton X-100, and insoluble material pelleted by centrifugation at 100,000 × G for 30 min. Extracts were incubated with control amylose beads or amylose beads saturated with maltose-binding fusion proteins as indicated. Samples were loaded into disposable columns, which were washed with 50 volumes of buffer containing 1% Triton X-100 + 300 mM NaCl. Retained proteins were eluted with 150 µl of loading buffer and were resolved by SDS-PAGE. Blots were hybridized with a monoclonal antibody to nNOS (Transduction Labs, Lexington, KY).

Acknowledgments

We thank Wendell Lim at the University of California, San Francisco for circular dichroism analysis of nNOS PDZ domains; Philip Hieter at Johns Hopkins School of Medicine and Mark Boguski at the National Center for Biotechnology Information for letting us use the prereleased XREFPatScan software; Gordon Ringold, Ronald Barrett, and William Dower at Affymax Research Institute for their support; and Xiao-dong Li for GST-NAB_{HERG} protein and helpful advice. We also thank Robyne Butzner for helping with manuscript preparation. This work is supported by grants (to ML) from the National Institutes of Health, the Muscular Dystrophy Association, the American Heart Association-Pfizer award, and the Council for Tobacco Research, USA, Inc., and by grants (to DSB) from the National Institutes of Health, the Muscular Dystrophy Association, the McKnight Endowment, and the Lucille P. Markey Charitable Trust.

1. Cho, K.O., Hunt, C.A., and Kennedy, M.B. 1992. The rat brain postsynaptic density fraction contains a homolog of the *Drosophila* discs-large tumor suppressor protein. *Neuron* **9**:929-42.
2. Gomperts, S.N. 1996. Clustering membrane proteins: it is all coming

- together with the PSD-95/SAP90 protein family. *Cell* **84**:659-662.
3. Ponting, C.P. and Phillips, C. 1995. DHR domains in syntrophins, neuronal NO synthases and other intracellular proteins. *Trends Biol. Sci.* **20**:102-103.
4. Kim, E., et al. 1995. Clustering of Shaker-type K⁺ channels by direct interaction with the PSD-95/SAP90 family of membrane-associated guanylate kinases. *Nature* **378**:85-88.
5. Kornau, H.-C., Schenker, L.T., Kennedy, M.B., and Seeburg, P.H. 1995. Domain interaction between NMDA receptor subunits and the postsynaptic density protein PSD-95. *Science* **269**:1737-1740.
6. Sheng, M. 1996. PDZs and receptor/channel clustering: rounding up the latest suspects. *Neuron* **17**:575-578.
7. Doyle, D.A., Lee, A., Lewis, J., Kim, E., Sheng, M., and MacKinnon, R. 1996. Crystal structures of a complexed and peptide-free membrane protein-binding domain: molecular basis of peptide recognition by PDZ. *Cell* **85**:1067-1076.
8. Cabral, J.H.M., et al. 1996. Crystal structure of a PDZ domain. *Nature* **382**:649-652.
9. Muller, B.M., Kistner, U., Kindler, S., Chung, W.K., Kuhlendahl, S., Fenster, S.D., et al. 1996. SAP102, a novel postsynaptic protein that interacts with NMDA receptor complexes in vivo. *Neuron* **17**:255-265.
10. Cohen, N.A., Brenman, J.E., Snyder, S.H., and Bredt, D.S. 1996. Binding of the inward rectifier K⁺ channel to PSD-95 is regulated by protein kinase A phosphorylation. *Neuron* **17**:759-767.
11. Bredt, D.S. and Snyder, S.H. 1994. Nitric oxide: a physiologic messenger molecule. *Ann. Rev. Biochem.* **63**:175-195.
12. Marletta, M.A. 1993. Nitric oxide synthase structure and mechanism. *J. Biol. Chem.* **268**:12231-4.
13. Moncada, S. and Higgs, A. 1993. The L-arginine-nitric oxide pathway. *N. Engl. J. Med.* **329**:2002-2012.
14. Dawson, T.M., Dawson, V.L., and Snyder, S.H. 1992. A novel neuronal messenger molecule in brain: the free radical, nitric oxide [see comments]. *Ann. Neurol.* **32**:297-311.
15. Hantraye, P., Brouillet, E., Ferrante, R., Palfi, S., Dolan, R., Matthews, R.T., et al. 1996. Inhibition of neuronal nitric oxide synthase prevents MPTP-induced parkinsonism in baboons. *Nature Medicine* **2**:1017-1021.
16. Huang, Z., Huang, P.L., Panahian, N., Dalkara, T., Fishman, M.C., and Moskowitz, M.A. 1994. Effects of cerebral ischemia in mice deficient in neuronal nitric oxide synthase. *Science* **265**:1883-1885.
17. Jaffrey, S.R. and Snyder, S.H. 1996. PIN: An associated protein inhibitor of neuronal nitric oxide synthase. *Science* **274**:774-777.
18. Aoki, C., Fenstermaker, S., Lubin, M., and Go, C.G. 1993. Nitric oxide synthase in the visual cortex of macaque monkeys as revealed by light and electron microscopic immunocytochemistry. *Brain Res.* **620**:97-113.
19. Brenman, J.E., Chao, D.S., Xia, H., Aldape, K., and Bredt, D.S. 1995. Nitric oxide synthase complexed with dystrophin and absent from skeletal muscle sarcolemma in Duchenne muscular dystrophy. *Cell* **82**:743-752.
20. Brenman, J.E., Chao, D.S., Gee, S.H., McGee, A.W., Craven, S.E., Santillano, D.R., et al. 1996. Interaction of nitric oxide synthase with the synaptic density protein PSD-95 and α-1 syntrophin mediated by PDZ motifs. *Cell* **84**:757-767.
21. Brenman, J.E., Christopherson, K.S., Craven, S.E., McGee, A.W., and Bredt, D.S. 1996. Cloning and characterization of postsynaptic density 93, PSD-93, a nitric oxide synthase interacting protein. *J. Neurosci.* **16**:7407-7415.
22. Chao, D.S., Gorospe, R.M., Brenman, J.E., Rafael, J.A., Peters, M.F., Froehner, S.C., et al. 1996. Selective loss of sarcolemmal nitric oxide synthase in Becker muscular dystrophy. *J. Exp. Med.* **184**:609-618.
23. Sparks, A.B., Adey, N.B., Quilliam, L.A., Thorn, J.M., and Kay, B.K. 1995. Screening phage-displayed random peptide libraries for SH3 ligands. *Methods Enzymol.* **255**:498-509.
24. Zhou, S. and Cantley, L.C. 1995. SH2 domain specificity determination using oriented phosphopeptide library. *Methods Enzymol.* **254**:523-535.
25. Gallop, M., Barrett, R., Dower, W., Fodor, S., and Gordon, E. 1994. Applications of combinatorial technologies to drug discovery. 1. Background and peptide combinatorial libraries. *J. Med. Chem.* **37**:1233-1251.
26. Cull, M.G., Miller, J.F., and Schatz, P.J. 1992. Screening for receptor ligands using large libraries of peptides linked to the C terminus of the lac repressor. *Proc. Natl. Acad. Sci. USA* **89**:1865-1869.
27. Niethammer, M., Kim, E., and Sheng, M. 1996. Interaction between the C terminus of NMDA receptor subunits and multiple members of the PSD-95 family of membrane-associated guanylate kinases. *J. Neurosci.* **16**:2157-2163.
28. Bredt, D.S., Hwang, P.M., Glatt, C.E., Lowenstein, C., Reed, R.R., and Snyder, S.H. 1991. Cloned and expressed nitric oxide synthase structurally resembles cytochrome P-450 reductase. *Nature* **351**:714-718.
29. Schatz, P.J., Cull, M.G., Martin, E.L., and Gates, C.M. 1996. Screening of peptide libraries linked to lac repressor. *Methods Enzymol.* **267**:171-191.
30. Garthwaite, J., Charles, S.L., and Chess-Williams, R. 1988. Endothelium-derived relaxing factor release on activation of NMDA receptors suggests role as intercellular messenger in the brain. *Nature* **336**:385-388.
31. Vesely, D.L. 1981. Melatonin enhances guanylate cyclase activity in a variety of tissues. *Mol. Cell Biochem.* **35**:55-58.
32. Garthwaite, J. and Boulton, C.L. 1995. Nitric oxide signaling in the central nervous system. *Annu. Rev. Physiol.* **57**:683-706.
33. Richarme, G. 1982. Associative properties of the *Escherichia coli* galactose binding protein and maltose binding protein. *Biochem. Biophys. Res. Comm.* **105**:476-481.
34. Fields, S. and Song, S.-K. 1989. A novel genetic system to detect protein-protein interactions. *Nature* **340**:245-246.
35. Li, X.-D., Xu, J., and Li, M. 1997. The human Δ1261 mutation of the HERG potassium channel results in a truncated protein that contains a subunit interaction domain and decreases the channel expression. *J. Biol. Chem.* **272**:705-708.